Applied Surface Science 428 (2018) 793–797

Contents lists available at ScienceDirect

Applied Surface Science

journal homepage: www.elsevier.com/locate/apsusc

Full Length Article

Selenidation of epitaxial silicene on ZrB_2

F.B. Wiggers[a,*], Y. Yamada-Takamura[b], A.Y. Kovalgin[a], M.P. de Jong[a]

[a] MESA+ Institute for Nanotechnology, University of Twente, 7500 AE Enschede, The Netherlands
[b] School of Materials Science, Japan Advanced Institute of Science and Technology, Nomi, Ishikawa, 923-1292, Japan

ARTICLE INFO

Article history:
Received 5 July 2017
Received in revised form 1 September 2017
Accepted 20 September 2017
Available online 20 September 2017

Keywords:
Silicene
Selenium
Transition metal diboride
Low-energy electron diffraction
Photoelectron spectroscopy

ABSTRACT

The deposition of elemental Se on epitaxial silicene on ZrB_2 thin films was investigated with synchrotron-based core-level photoelectron spectroscopy and low-energy electron diffraction. The deposition of Se at room temperature caused the appearance of Si 2*p* peaks with chemical shifts of $n \times 0.51 \pm 0.04$ eV (n = 1-4), suggesting the formation of $SiSe_2$. This shows that capping the silicene monolayer, without affecting its structural and electronic properties, is not possible with Se. The annealing treatments that followed caused the desorption of Se and Si, resulting in the etching of the Si atoms formerly part of the silicene layer, and the formation of bare $ZrB_2(0001)$ surface area. In addition, a $ZrB_2(0001)$-$(\sqrt{7} \times 3)$R40.9° surface reconstruction was observed, attributed to a Se-termination of the surface of the transition metal diboride thin film.

1. Introduction

Silicene is a two-dimensional (2D) material with an atomically buckled, honeycomb lattice of Si atoms [1]. This material is predicted to exhibit charge carriers that behave as massless Dirac fermions [1], and the quantum spin Hall effect [2]. Due to the relatively weak π-bonds of silicene, the surface is more chemically reactive than that of e.g. graphene. This currently restricts the characterization and processing of epitaxial silicene to vacuum systems that are also capable of *in situ* synthesis, or requires sample transport after synthesis to another system without breaking the vacuum. A capping layer of Se is commonly used for Se-based 2D materials, such as WSe_2 and $MoSe_2$, and can be desorbed again by annealing at 200 °C [3]. This motivated us to investigate Se as a capping layer for epitaxial silicene on ZrB_2 thin films.

In the current work, Se was deposited on epitaxial silicene on $ZrB_2(0001)$ thin films on Si(111) substrates at room temperature, and subsequently annealed up to 600 °C. The chemical composition and ordering of the surface was measured after both deposition and several annealing steps using synchrotron-based high-resolution photoelectron spectroscopy (HR-PES) and low-energy electron diffraction (LEED), respectively.

2. Experimental

Single-crystalline ZrB_2 epitaxial thin films were grown on Si(111) substrates by ultra-high vacuum chemical vapor epitaxy which is described elsewhere [4]. All subsequent sample preparation steps and measurements were performed at the MatLine beamline of the ASTRID2 synchrotron at Aarhus University, Denmark. The endstation consists of a loadlock (base pressure 7×10^{-8} mbar), and an analysis chamber (base pressure 4×10^{-10} mbar) equipped with a Scienta SES200 hemispherical analyzer for HR-PES measurements. Annealing is carried out in the analysis chamber by means of direct e-beam heating on the backside of the sample through a hole in the sample plate, while the temperature is measured using a thermocouple, and a pyrometer for temperatures of 600 °C and above. The same chamber is also equipped with a LEED system. The loadlock is equipped with a Se deposition source.

Sample preparation involves annealing at 800 °C in ultra-high vacuum, which is known to terminate the surface with a monolayer of silicene, with the Si originating from the Si substrate [5]. Following sample preparation, the samples were investigated *in situ* by LEED and HR-PES. All HR-PES measurements were carried out with the sample normal directed towards the photoelectron analyzer and with the photon source at a 45° angle to the surface normal.

The binding energy scale of the Si 2*p* spectrum of the pristine ZrB_2 surface, measured with a photon energy of 150 eV, was calibrated using the dominant Si $2p_{3/2}$ peak at 98.98 eV of epitaxial silicene on ZrB_2 [6]. The same calibration offset was applied to all other Si 2*p* spectra. The binding energy scale of the B 1*s* and Zr 3*d*

* Corresponding author.
E-mail address: F.B.Wiggers@utwente.nl (F.B. Wiggers).

http://dx.doi.org/10.1016/j.apsusc.2017.09.167
0169-4332/

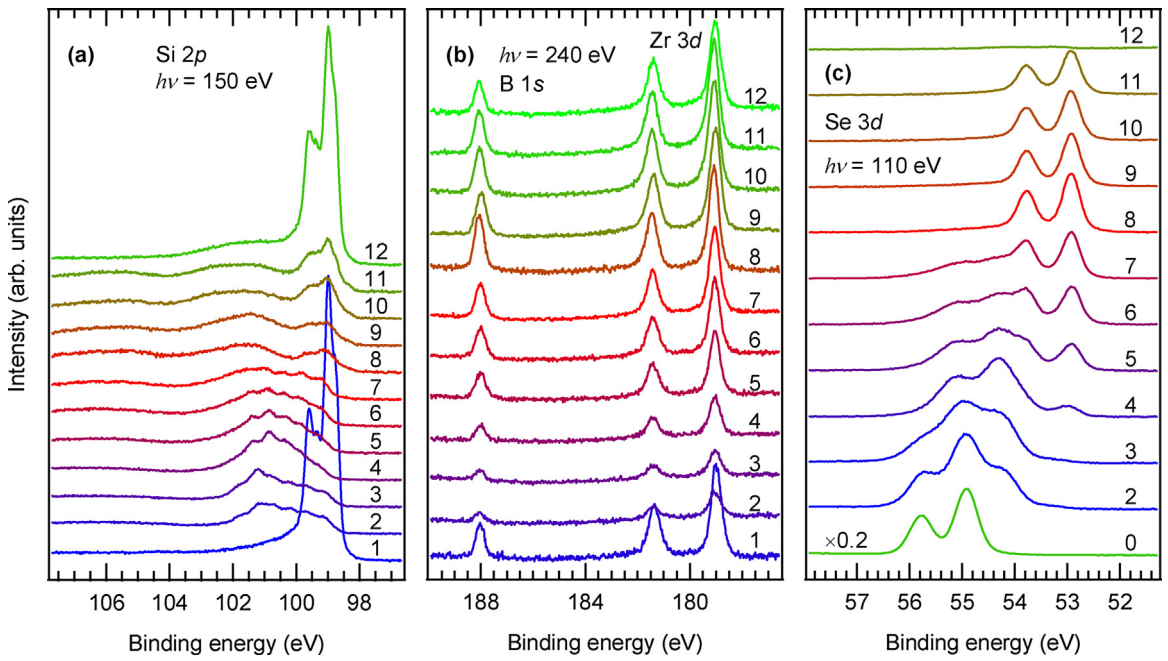

Fig. 1. High-resolution photoelectron spectra of (a) Si 2*p*, (b) B 1*s* and Zr 3*d*, and (c) Se 3*d* core-level regions of the silicene-terminated ZrB_2 surface before and after Se deposition and several annealing treatments. The spectra are presented in chronological order: (1) pristine silicene-terminated ZrB_2, (2) deposition of 0.5 nm Se, (3) after 11 h, (4) annealing to 340 °C, (5) annealing to 390 °C, (6) repeated, (7) annealing to 410 °C, (8) annealing to 470 °C, (9) repeated and 14 h later, (10) annealing at 470 °C for 10 min, (11) annealing to 500 °C, (12) annealing to 600 °C. Spectrum (0) is included for the Se 3*d* core level and serves as a reference for the bulk Se peak.

spectrum of the pristine ZrB_2 surface, measured using a photon energy of 240 eV, has been calibrated using values for the Zr $3d_{3/2}$ and Zr $3d_{5/2}$ peaks of 181.4 eV and 179.0 eV, respectively, corresponding to Zr atoms in a silicene-terminated $ZrB_2(0001)$ thin film. The same calibration offset has also been applied to all other B 1*s* and Zr 3*d* spectra. The Se 3*d* spectra were measured using a photon energy of 110 eV. The Se 3*d* binding energy scale was calibrated using the error found by linear extrapolation using the errors in the binding energy scales of the Si 2*p* and Zr 3*d* spectra. For Se 3*d* spectra 8–11 in Fig. 1(c) an error remained and these spectra were recalibrated based on the position of the main Se 3*d* component in spectrum 7. All spectra were normalized, after subtraction of the detector noise-level, on the signal intensity in the low binding-energy region.

The Se deposition source consists of a glass lightbulb with an opening at the top and a Ta shroud wrapped around it, to which a thermocouple is attached. It operates by thermal evaporation of Se powder (≥99.99% purity, MaTecK) contained within. Se deposition is carried out by exposing the sample surface, held within line-of-sight of the source opening at a distance of approximately 10 cm, at room temperature to the Se flux with a background pressure of 7×10^{-8} mbar. We note that the actual sample temperature was slightly higher than room temperature due to radiative heating from the source. Previous mass spectrometry studies have shown that solid Se vaporizes as Se_n (n = 2-9) species, with Se_6 in the highest abundance in the vapor [7,8].

3. Results and discussion

After introduction of the sample into the ultra-high vacuum system, it was annealed at 800 °C to remove the native oxide and to prepare a silicene-terminated $ZrB_2(0001)$ surface. This is confirmed by the Si 2*p* spectrum, shown in Fig. 1(a)(spectrum 1), featuring the characteristic shape corresponding to epitaxial silicene on ZrB_2, as reported previously [5]. Peak fitting shows in Fig. 2(a)(spectrum 1) that the spectral envelope can be well explained by the presence of epitaxial silicene [9], together with a minor component attributed to Si sub-oxides remaining after the annealing treatment. In addition, the $ZrB_2(0001)$-(2×2) reconstruction is observed in the LEED measurements, as shown in Fig. 4(a), which is equivalent to the $(\sqrt{3} \times \sqrt{3})$-reconstruction of silicene. The Zr 3*d* and B 1*s* spectrum shown in Fig. 1(b)(spectrum 1) features a Zr 3*d* doublet, with the $3d_{3/2}$ and $3d_{5/2}$ peaks at 181.4 eV and 179.0 eV, and a B 1*s* peak, at 188.1 eV, corresponding to Zr and B atoms in the ZrB_2 thin film. In the following, this as-annealed surface is referred to as the pristine surface.

Subsequently, approximately 0.5 nm of Se was deposited in 10 min, with the substrate kept at room temperature. The amount of Se was estimated based on an overlayer-substrate model using the suppression of the Si 2*p* and Zr 3*d* core levels.

The Si 2*p* spectrum in Fig. 1(a)(spectrum 2) is suppressed and a wide distribution of chemical states is observed. Five components are resolved in the spectral envelope, and were further analyzed by peak fitting, as shown in Fig. 2(a)(spectrum 2). In this way, five major components were fitted, which were found to be equally spaced with an average interval of 0.51 ± 0.04 eV, and are positioned at 99.12 eV, 99.62 eV, 100.17 eV, 100.68 eV, and 101.14 eV binding energy, respectively. The five major components are of approximately equal intensity.

The disappearance of silicene-related components is explained by chemical bonding between the deposited Se and Si from the epitaxial silicene. Based on the notion that Si forms 4 covalent bonds, and the equal spacing of the Si 2*p* chemical shifts, these five major components can be attributed to $Si–Se_x$ (x = 0-4) species, suggesting the formation of $SiSe_2$. Bringans *et al.* [10] observed a similar distribution of components in the Si 2*p* spectrum, with an interval for the chemical shift of 0.53 ± 0.03 eV, following Se deposition on a Si(100) surface and an annealing treatment at 300 °C. An analogy can be made with SiO_2 and its sub-oxides [11].

The deposition of Se is confirmed by the appearance of Se 3*d* peaks, shown in Fig. 1(c)(spectrum 2). Peak fitting revealed two major components and a minor third component as shown in Fig. 2(b)(spectrum 2). In a separate experiment, an amount of Se of at least three times more was deposited on the same sample

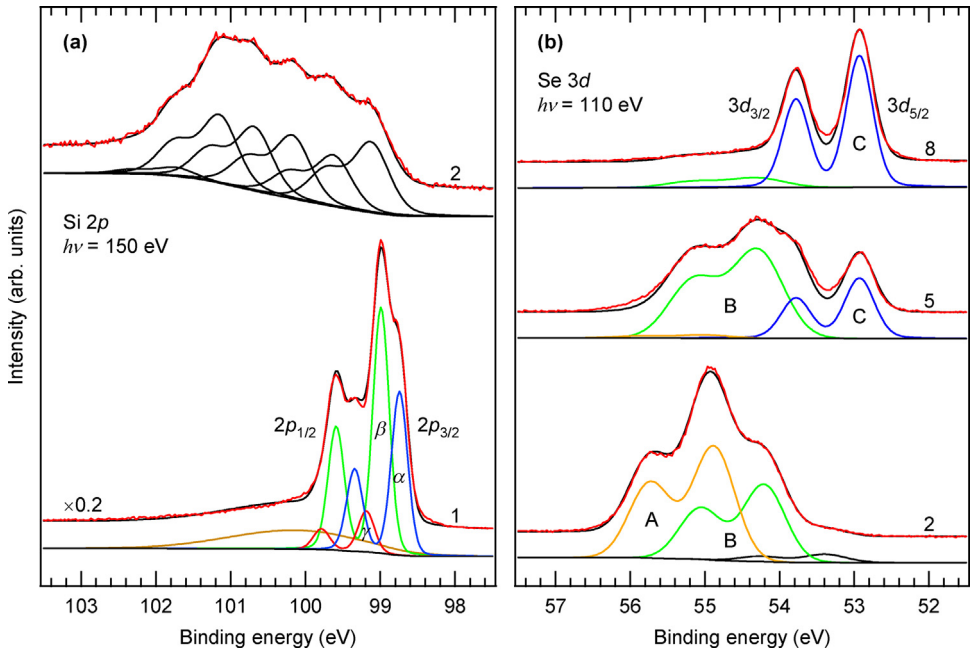

Fig. 2. Peak fitting of (a) Si 2*p*, and (b) Se 3*d* spectra. The spectrum number corresponds to the identification given in Figs. 1(a) and (c). The components identified in these spectra represent the most significant chemical states that are necessary to discuss the recorded spectra of Figs. 1(a) and (c). The sum of the fitted data (black) is plotted behind the measured data (red), while the fitted components and the background are offset below. The Si 2*p* spectra were peak fitted using a Shirley background and symmetric Gaussian line shapes for spectrum 1, and line shapes based on a Gaussian-Lorentzian sum function with a 76% Gaussian character for spectrum 2. Each component consists of a doublet with an area ratio of 1:2 for the Si $2p_{1/2}$ and Si $2p_{3/2}$ peaks, respectively, and 0.6 eV spin-orbit splitting. The peak model for silicene is based on the lattice model of epitaxial silicene on the ZrB_2 surface [5], characterized by three unique atomic sites occupied by Si atoms, that correspond to the components α, β, and γ, which occur in the ratio 2:3:0.5 [9]. The components were fitted with a distance of 230 meV between α and β, and 160 meV between β and γ, and with a full width at half maximum (FWHM) of 256 meV. The Se 3*d* spectra were peak fitted using a Shirley background and symmetric Gaussian line shapes for components A and B, and a line shape based on a Gaussian-Lorentzian sum function with an 85% Gaussian character for component C. Each component consists of a doublet with an area ratio of 2:3 for the Se $3d_{3/2}$ and Se $3d_{5/2}$ peaks, respectively, and 0.85 eV spin-orbit splitting. (For interpretation of the references to colour in this figure legend, the reader is referred to the web version of this article.)

in order to identify the bulk Se peak, shown in Fig. 1(c)(spectrum 0). Based on the comparison, component A at a binding energy of 54.88 eV is attributed to bulk Se. Component B at a binding energy of 54.21 eV is attributed to $SiSe_x$ species. This is further supported by the disappearance of the A component upon annealing, as will be discussed later, while the B component remains, together with the five major Si 2*p* components.

The B 1*s* and Zr 3*d* peaks shown in Fig. 1(b)(spectrum 2) are suppressed, but do not show an indication of newly-formed peaks, suggesting that the ZrB_2 substrate is not strongly interacting with the deposited Se.

11 h after Se deposition, with the sample kept in the analysis chamber at room temperature, the Se 3*d* spectrum was measured and shows a decrease in intensity for component A and an increase for component B, as shown in Fig. 1(c)(spectrum 3), while the total Se 3*d* intensity remains nearly constant, as shown in Fig. 3. The Si 2*p* spectrum shows an increase for the highest component, associated with $SiSe_2$. This suggests a slowly progressing solid-phase reaction at room temperature between the deposited Se and Si.

Subsequently, in order to investigate the behavior of Se on the Si-terminated ZrB_2 surface, the sample was heated to progressively higher temperatures of up to 600 °C, while monitoring the Se 3*d* spectrum *in situ*. At several points the heating was stopped and the sample was allowed to cool down to room temperature in order to acquire HR-PES spectra and perform LEED measurements. For temperatures below 600 °C, the temperature was measured using a thermocouple. For 600 °C and above, a pyrometer was used. As the thermocouple is mounted on the sample plate, while the sample is heated directly by e-beam heating, a difference between the reading of the thermocouple and the actual sample temperature can be

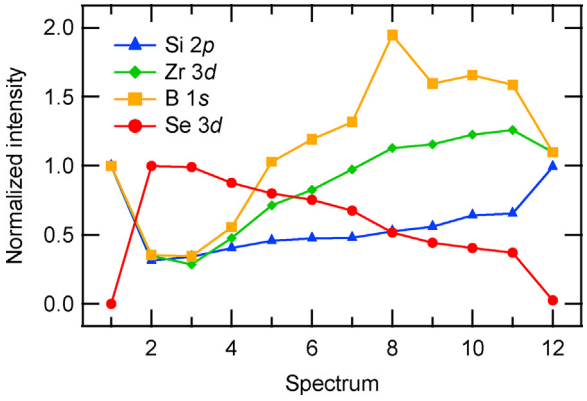

Fig. 3. The normalized intensities of the Si 2*p*, Zr 3*d*, B 1*s*, and Se 3*d* core levels. The spectrum number corresponds to the identification given in Fig. 1.

expected. In the case of the 600 °C reading by the pyrometer, the thermocouple measured 550 °C.

Component A continues to decrease in intensity upon heating the sample, and disappears upon reaching 340 °C, as shown in Fig. 1(c)(spectrum 4), while component B remains. Simultaneously, a new Se 3*d* peak appears at a lower binding energy at 53.0 eV. Furthermore, a faint ZrB_2-(1×1) pattern can be observed by LEED, as shown in Fig. 4(b), while the silicene-related diffraction spots have disappeared. In addition, the distance in binding energy between the B 1*s* and Zr 3*d* core levels decreases gradually, starting with the deposition of Se and saturating at a total decrease of 70 meV after annealing at 340 °C.

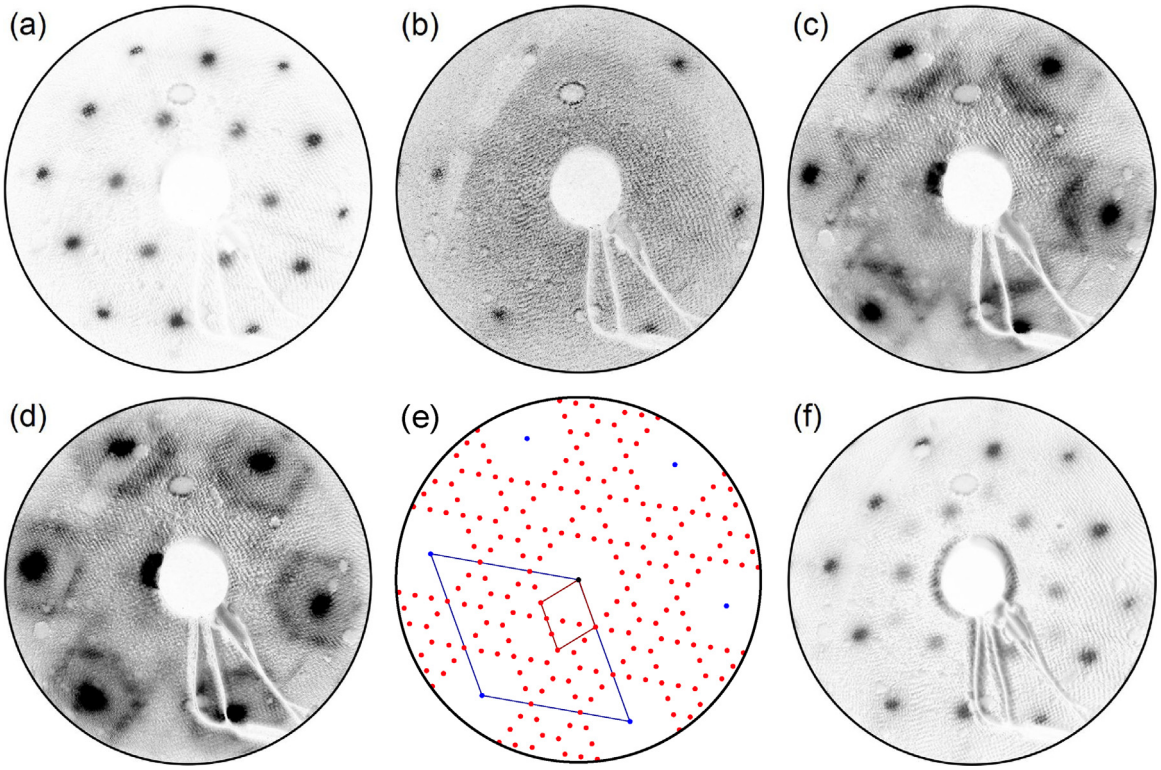

Fig. 4. LEED patterns of the (a) pristine silicene-terminated $ZrB_2(0001)$-(2×2) surface, (b) after Se deposition and annealing at 340 °C (corresponding to spectrum 4 in Fig. 1), (c), (d) after annealing at 470 °C (corresponding to spectrum 8 in Fig. 1), and (f) after annealing at 600 °C (corresponding to spectrum 12 in Fig. 1). The LEED patterns (a), (b), (c), and (f) were recorded with $E = 50$ eV, (d) with $E = 55$ eV. The observed pattern in (c) and (d) matches with (e) a $(\sqrt{7} \times 3)$R40.9° reconstruction of the $ZrB_2(0001)$ surface, consisting of six rotated domains. The (1×1) and $(\sqrt{7} \times 3)$R40.9° unit cells of $ZrB_2(0001)$ are shown in reciprocal space in dark blue and dark red, respectively. The clarity of the images was improved in post-processing by subtraction of a recorded diffuse background. The spot immediately left of the electron gun in (c) and (d) is a reflection of the filament. (For interpretation of the references to colour in this figure legend, the reader is referred to the web version of this article.)

The total Se 3*d* intensity steadily decreases upon annealing to 390 °C, 410 °C, and 470 °C, while the intensities of Si 2*p*, Zr 3*d*, and B 1*s* increase, as shown in Fig. 3(spectra 2–9). Interestingly, the intensities of Zr 3*d* and B 1*s* increase more rapidly compared to Si 2*p* and exceed their pristine-surface intensities. It is noted that the B 1*s* intensity measured for spectrum 8 is an outlier: spectrum 9 serves as an approximate replacement, acquired after only a repeated annealing treatment at 470 °C. Coinciding with annealing at 470 °C the Si 2*p* components associated with $SiSe_x$ species have disappeared, while a new feature has appeared at a similar binding energy as that of silicene, as shown in Fig. 1(a)(spectrum 8 and 9).

These results can be explained by the desorption of Se_n species [7,8,12] and $SiSe_x$ compounds, thereby removing Se, but also Si that was formerly part of the silicene monolayer terminating the ZrB_2 surface. This is in agreement with the reported desorption of Se, SiSe, and $SiSe_2$ from Si(100) surfaces with deposited Se, at temperatures as low as 330 °C for more than 2 ML of deposited Se [12,13]. Consequently, the amount of material on the surface is reduced, increasing the B 1*s* and Zr 3*d* intensities. These core levels exceed their pristine-surface intensities, suggesting that the combined coverage of the remaining Se and Si is less than that of the initial silicene monolayer, indicating the formation of bare ZrB_2 surface area. This is interesting for ZrB_2 thin films grown on Si(111) substrates, because, as was discussed earlier, the surface is either covered by native Si oxide, or silicene after annealing [5,14].

The new Si 2*p* feature is attributed to silicene and can be explained by the incomplete etching of the Si, allowing the remaining Si to recrystallize as silicene on the $ZrB_2(0001)$ surface. A comparison of the intensity of the feature in spectrum 8 of Fig. 1(a) with that of the pristine silicene in spectrum 1, suggests the surface coverage of the recrystallized silicene to be about 6% compared to the pristine surface coverage. The recrystallization of silicene at these temperatures is supported by the reported formation of silicene by Si deposition on bulk $ZrB_2(0001)$ at temperatures lower than 300 °C [15]. In addition, Fleurence *et al.* [14] reported recrystallization of silicene at 450 °C following a sputtering treatment of the silicene-terminated $ZrB_2(0001)$ surface by Ar^+ bombardment.

Component B in the Se 3*d* spectra steadily diminishes upon annealing, while the new peak increases, and finally is the only peak remaining, as shown in Fig. 1(c)(spectra 5–9). The new Se 3*d* peak at 52.93 eV binding energy was identified as component C by peak fitting, shown in Fig. 2(b)(spectra 5 and 8).

After annealing at 390 °C and 410 °C, a faint, new pattern appears as observed by LEED, in addition to the ZrB_2-(1×1) reconstruction. The new pattern is most intense after annealing at 470 °C and corresponds to $ZrB_2(0001)$-$(\sqrt{7} \times 3)$R40.9°, as shown in Figs. 4(c–e), and was acquired together with HR-PES spectra series 8, shown in Figs. 1(a–c). This coincides with the disappearance of the B component, while component C remains. The surface reconstruction is likely caused by Se atoms on the $ZrB_2(0001)$ surface, made possible by the desorption of $SiSe_x$ species, thereby removing Si atoms and exposing bare ZrB_2 surface area. This is supported by the narrower FWHM of Se component C compared to B, indicating a higher degree of atomic order, and the disappearance of $SiSe_x$-related components. In addition, the lower binding energy of component C can be explained by the high electronegativity of Se relative to Zr. This means it is a good electron acceptor and it could attract some electron density from the Zr substrate atoms. It is noted that the surface of clean $ZrB_2(0001)$ is (1×1) [15,16].

An atomistic model of the reconstructed surface cannot be unambiguously assigned based purely on the LEED pattern. Previously reported STM studies of electrodeposited Se on Ag(111)

[17] and Au(111) [18] showed that Se can adsorb on the surface as highly ordered adatom decorations, or form adlayers of square rings of Se_8.

It is suggested that annealing the ZrB_2 thin film surface while simultaneously depositing Se could allow for complete removal of the silicene monolayer. Selection of an appropriate temperature for the Se source and sample, with the aim of ensuring a self-limiting adsorption of only a monolayer [12], could then fully terminate the $ZrB_2(0001)$ surface with Se in a highly ordered manner.

Annealing at 470 °C for 10 min, and then at 500 °C, continues the trend of increasing intensities for B 1*s*, Zr 3*d*, and Si 2*p*, and a decrease for Se 3*d*, as shown in Fig. 3(spectrum 10–11). For the final annealing temperature of 600 °C, the B 1*s*, Zr 3*d*, and Si 2*p* core levels return to their pristine-surface intensities, while the Se 3*d* peak nearly disappears, as shown in Fig. 3. The Si 2*p* spectrum is now very similar to that of the pristine surface, as shown in Fig. 1(a)(spectrum 1 and 12). This can be explained by the desorption of remaining Se from the ZrB_2 surface, and the formation of a silicene monolayer by segregation of Si from the Si substrate. This is in agreement with a previous report of surface segregation of Si atoms at a temperature of 600 °C on the surface of a $ZrB_2(0001)$ thin film on a Si(111) substrate, resulting in the formation of a silicene layer [14]. The reappearance of the ZrB_2-(2×2) pattern, equivalent to the silicene-$(\sqrt{3} \times \sqrt{3})$ pattern, as observed by LEED in Fig. 4(f), further supports this. In addition, the distance in binding energy between the B 1*s* and Zr 3*d* core levels, which decreased upon deposition of Se and annealing, as discussed earlier, has suddenly increased, back to a value similar to that of the pristine surface. This can be explained by the removal and restoration of the Si interaction with the outer Zr atoms that terminate the ZrB_2 thin film [5,14], resulting respectively in an increase and decrease of the binding energy of the surface-related Zr 3*d* peak. The physical principle that causes such changes is the redistribution of the valence electrons and the corresponding electron density in the Zr atoms, which changes the screening of the 3*d* core levels, and consequently their binding energy.

It is noted that there are two broad features in the Si 2*p* spectra in Fig. 1(a), centered at approximately 101.5-102.0 eV (spectra 8–12), and 106.5 eV (spectra 2–11). The latter feature can be explained as a loss feature, caused by inelastic scattering of Si 2*p* photoelectrons. The feature at 101.5-102.0 eV can be explained by Si sub-oxide or remaining $SiSe_x$ species.

Further, it is noted that the intensity of the B 1*s* core level, shown in Fig. 3, follows the same trend as that of the Zr 3*d* core level, however after annealing to 390 °C it is relatively more intense until the surface is again terminated with a silicene monolayer. This can possibly be explained by photoelectron diffraction involving the silicene layer.

4. Conclusions

Deposition of Se at room temperature on epitaxial silicene on $ZrB_2(0001)$ thin films resulted in chemical bonding between the deposited Se and Si from silicene. The silicene-related Si 2*p* peaks disappeared, while new components appeared, equally spaced by an average interval of 0.51 ± 0.04 eV, suggesting the formation of $SiSe_2$ and intermediate species. Capping of the silicene surface, without affecting its structural and electronic properties, is therefore not possible with Se.

The progression of the relative intensities of the Si 2*p*, B 1*s*, and Zr 3*d* core levels during annealing of the sample with deposited Se up to 470 °C, indicates the desorption of Se and Si, thereby etching the Si atoms formerly part of the silicene monolayer. This resulted in the formation of bare $ZrB_2(0001)$ surface area coexisting with a novel surface reconstruction, attributed to Se-terminated $ZrB_2(0001)$-$(\sqrt{7} \times 3)$R40.9°. The Se was removed by annealing to 600 °C, which also resulted in the simultaneous restoration of the silicene monolayer by Si originating from the Si substrate.

Acknowledgements

This work is part of the research program of the Foundation for Fundamental Research on Matter (FOM, Grant No. 12PR3054), which is part of the Netherlands Organization for Scientific Research (NWO). We thank ISA at Aarhus University, Denmark, for providing synchrotron beam time. We also thank J. Schmitz for suggestions that improved the manuscript. Y.Y.-T. acknowledges support from JSPS KAKENHI Grant Number JP26246002.

References

[1] S. Cahangirov, M. Topsakal, E. Aktürk, H. Şahin, S. Ciraci, Two- and One-Dimensional Honeycomb Structures of Silicon and Germanium, Phys. Rev. Lett. 102 (2009) 236804.
[2] C.-C. Liu, W. Feng, Y. Yao, Quantum spin hall effect in silicene and two-dimensional germanium, Phys. Rev. Lett. 107 (2011) 76802.
[3] H.J. Liu, L. Jiao, L. Xie, F. Yang, J.L. Chen, W.K. Ho, C.L. Gao, J.F. Jia, X.D. Cui, M.H. Xie, Molecular-beam epitaxy of monolayer and bilayer WSe_2: a scanning tunneling microscopy/spectroscopy study and deduction of exciton binding energy, 2D Mater. 2 (2015) 34004.
[4] Y. Yamada-Takamura, F. Bussolotti, A. Fleurence, S. Bera, R. Friedlein, Surface electronic structure of ZrB_2 buffer layers for GaN growth on Si wafers, Appl. Phys. Lett. 97 (2010) 73109.
[5] A. Fleurence, R. Friedlein, T. Ozaki, H. Kawai, Y. Wang, Y. Yamada-Takamura, Experimental evidence for epitaxial silicene on diboride thin films, Phys. Rev. Lett. 108 (2012) 245501.
[6] R. Friedlein, A. Fleurence, K. Aoyagi, M.P. de Jong, H. Van Bui, F.B. Wiggers, S. Yoshimoto, T. Koitaya, S. Shimizu, H. Noritake, K. Mukai, J. Yoshinobu, Y. Yamada-Takamura, Core level excitations—A fingerprint of structural and electronic properties of epitaxial silicene, J. Chem. Phys 140 (2014) 184704.
[7] H. Fujisaki, J.B. Westmore, A.W. Tickner, Mass spectrometric study of subliming selenium, Can. J. Chem. 44 (1966) 3063–3071.
[8] R. Viswanathan, R. Balasubramanian, D. Darwin Albert Raj, M. Sai Baba, T.S. Lakshmi Narasimhan, Vaporization studies on elemental tellurium and selenium by Knudsen effusion mass spectrometry, J. Alloys Compd. 603 (2014) 75–85.
[9] C.-C. Lee, J. Yoshinobu, K. Mukai, S. Yoshimoto, H. Ueda, R. Friedlein, A. Fleurence, Y. Yamada-Takamura, T. Ozaki, Single-particle excitation of core states in epitaxial silicene, Phys. Rev. B. 95 (2017) 115437.
[10] R.D. Bringans, M.A. Olmstead, Bonding of Se and ZnSe to the Si(100) surface, Phys. Rev. B. 39 (1989) 12985–12988.
[11] Z.H. Lu, M.J. Graham, D.T. Jiang, K.H. Tan, SiO_2/Si(100) interface studied by Al Kα x-ray and synchrotron radiation photoelectron spectroscopy, Appl. Phys. Lett. 63 (1993) 2941–2943.
[12] M. Tao, E. Maldonado, W.P. Kirk, Monolayer passivation of silicon(001) surface by selenium, Appl. Surf. Sci. 253 (2007) 4578–4580.
[13] A.C. Papageorgopoulos, M. Kamaratos, Adsorption and desorption of Se on Si(100)2×1: surface restoration, Surf. Sci. 466 (2000) 173–182.
[14] A. Fleurence, Y. Yamada-Takamura, Insights into the spontaneous formation of silicene sheet on diboride thin films, Appl. Phys. Lett. 110 (2017) 41601.
[15] T. Aizawa, S. Suehara, S. Otani, Phonon dispersion of silicene on $ZrB_2(0001)$, J. Phys. Condens. Matter. 27 (2015) 305002.
[16] T. Aizawa, W. Hayami, S. Otani, Surface phonon dispersion of $ZrB_2(0001)$ and $NbB_2(0001)$, Phys. Rev. B. 65 (2001) 24303.
[17] M. Cavallini, G. Aloisi, R. Guidelli, An in situ STM study of selenium electrodeposition on Ag(111), Langmuir 15 (1999) 2993–2995.
[18] T.E. Lister, J.L. Stickney, Atomic level studies of selenium electrodeposition on gold(111) and gold(110), J. Phys. Chem. 100 (1996) 19568–19576.